

## High-pressure crystal chemistry of Fe<sup>3+</sup>-wadsleyite, $\beta$ -Fe<sub>2.33</sub>Si<sub>0.67</sub>O<sub>4</sub>

ROBERT M. HAZEN,\* HEXIONG YANG, AND CHARLES T. PREWITT

Geophysical Laboratory and Center for High Pressure Research, Carnegie Institution of Washington, 5251 Broad Branch Road, N.W., Washington, D.C. 20015-1305, U.S.A.

### ABSTRACT

The crystal structure of Fe<sup>3+</sup>-wadsleyite, (Fe<sub>1.67</sub><sup>2+</sup>Fe<sub>0.33</sub><sup>3+</sup>)(Fe<sub>0.33</sub><sup>3+</sup>Si<sub>0.67</sub>)O<sub>4</sub>, was determined by single-crystal X-ray techniques at six pressures to 8.95 GPa. The isothermal bulk modulus is  $K_{70} = 173(3)$  GPa [ $K_{70} = \partial K_T / \partial P = 5.2(9)$ ], which is identical within error to bulk moduli observed for normal wadsleyites [ $\beta$ -(Mg,Fe)<sub>2</sub>SiO<sub>4</sub>]. Compression of Fe<sup>3+</sup>-wadsleyite is significantly more isotropic than for  $\beta$ -(Mg,Fe)<sub>2</sub>SiO<sub>4</sub> because Fe<sup>3+</sup> substitutes into both Si<sup>4+</sup> tetrahedral sites and (Mg,Fe<sup>2+</sup>) octahedral sites. Ferric iron thus reduces the contrast between tetrahedral and octahedral compressibilities, which in turn reduces the compressional anisotropy. Bond distance analysis and octahedral compressibilities of the three symmetrically distinct octahedral sites reveal that Fe<sup>3+</sup> orders preferentially into M1 and M3, while M2 occupancy is close to pure Fe<sup>2+</sup>.

### INTRODUCTION

Recent experiments on synthetic wadsleyite, which is nominally defined as  $\beta$ -(Mg,Fe)<sub>2</sub>SiO<sub>4</sub>, reveal structural and compositional complexities of considerable relevance to models of Earth's transition zone. Wadsleyite is the high-pressure polymorph of (Mg,Fe)<sub>2</sub>SiO<sub>4</sub> that lies between the stability fields of olivine (the lower-pressure  $\alpha$  form) and spinel (the higher-pressure  $\gamma$  form). As such, wadsleyite is presumed to be a major silicate phase in the upper transition zone, between about 410 and 500 km in depth (e.g., Anderson 1970; Jeanloz and Thompson 1983; Bina and Wood 1987; Ita and Stixrude 1992; Irifune and Isshiki 1998).

Unlike the structures of olivine and silicate spinel, the wadsleyite structure can accommodate significant amounts of hydrogen (Smyth 1987, 1994; Downs 1989; Bell and Rossman 1992; Young et al. 1993; Inoue 1994; Kudoh et al. 1996; Haiber et al. 1997) and trivalent cations (Smyth et al. 1997; Woodland and Angel 1998). These compositional variations are receiving considerable attention because they could cause alterations in the physical properties and expand the stability range of wadsleyite. These effects, in turn, could influence the sharpness and depth of seismic discontinuities associated with orthosilicate transitions in the mantle (e.g., Helfrich and Wood 1996; Fei and Bertka 1996). Wadsleyite compositional adaptability, furthermore, may play a significant role in defining the redox state and mechanisms of water transport associated with subduction zones (Kudoh et al. 1996; Woodland and Angel 1998; O'Neill et al. 1993; Kudoh and Inoue 1999). The addition of hydrogen, or hydrogen with trivalent cations, has been observed to result in a series of modified structures closely related to wadsleyite. Smyth et al. (1997) described (Mg<sub>1.73</sub>Fe<sub>0.10</sub>Al<sub>0.10</sub>Si<sub>0.99</sub>H<sub>0.36</sub>O<sub>4</sub>) with a wadsleyite-like unit cell, but monoclinic *I2/m* symmetry ( $\beta = 90.4^\circ$ ). Kudoh and Inoue (1999), similarly, report a monoclinic hydrous variant of wadsleyite (Mg<sub>1.86</sub>SiH<sub>0.28</sub>O<sub>4</sub>). Other related structures incorpo-

rate both wadsleyite- and spinel-like slabs to yield a homologous series of structures that share the  $\approx 6 \text{ \AA}$  *a* axis and  $\approx 8 \text{ \AA}$  *c* axes of wadsleyite, but differ in the *b* axis dimension, which is  $\approx 12 \text{ \AA}$  in wadsleyite (e.g., Ross et al. 1992; Smyth and Kawamoto 1997).

Substitution of ferric iron without hydrogen, on the other hand, yields wadsleyite isomorphs in which trivalent cations replace both octahedrally coordinated +2 and tetrahedrally coordinated +4 cations of the  $\beta$ -(Mg,Fe)<sub>2</sub>SiO<sub>4</sub> structure, without change of symmetry or unit-cell topology. Woodland and Angel (1998), for example, reported the synthesis and structure of  $\beta$ -(Fe<sub>1.55</sub><sup>2+</sup>Fe<sub>0.45</sub><sup>3+</sup>)(Fe<sub>0.45</sub><sup>3+</sup>Si<sub>0.55</sub>)O<sub>4</sub>, while Slesinger et al. (1997) and Ohtaka et al. (1997) synthesized similar wadsleyite isomorphs. The objective of the present study is to determine the compressibility and high-pressure crystal structure of the sample with composition (Fe<sub>1.67</sub><sup>2+</sup>Fe<sub>0.33</sub><sup>3+</sup>)(Fe<sub>0.33</sub><sup>3+</sup>Si<sub>0.67</sub>)O<sub>4</sub> synthesized by Slesinger et al., and to compare those results with similar data for  $\beta$ -(Mg,Fe)<sub>2</sub>SiO<sub>4</sub> (Hazen et al. 2000).

### EXPERIMENTAL PROCEDURES

The (Fe<sub>1.67</sub><sup>2+</sup>Fe<sub>0.33</sub><sup>3+</sup>)(Fe<sub>0.33</sub><sup>3+</sup>Si<sub>0.67</sub>)O<sub>4</sub> sample used in this study was synthesized at 6 GPa and 1200 °C at the Geophysical Laboratory's multi-anvil high-pressure laboratory by Slesinger et al. (1997). A single crystal (80 × 90 × 40  $\mu\text{m}^3$ ) was mounted in a modified Merrill-Bassett diamond-anvil cell with a mixture of 4:1 methanol:ethanol as the pressure medium. Three ruby chips (<10  $\mu\text{m}$ ) were included as the internal pressure calibrant (Mao et al. 1986), from which pressure was determined from the position of the R<sub>1</sub> laser-induced fluorescence peak, with an error of approximately 0.05 GPa.

A Picker four-circle diffractometer equipped with a Mo X-ray tube ( $\beta$ -filtered) was used for all X-ray diffraction measurements. The fixed- $\phi$  mode of data measurement (Finger and King 1978) was used throughout the high-pressure experiments to maximize reflection accessibility and minimize attenuation by the diamond cell. Unit-cell parameters were determined by fitting the positions of 14–16 reflections with  $20^\circ < 2\theta < 35^\circ$ , following the procedure of King and Finger (1979).

\*E-mail: hazen@gl.ciw.edu

X-ray diffraction intensity data were collected on the basis of the *I*-centered lattice for all accessible reflections with  $0 < 2\theta < 60^\circ$  using  $\omega$  scans of  $1^\circ$  width in step increments of  $0.025^\circ$  and 4s per step counting time. The intensity data were measured at six pressures up to 8.95 GPa. Digitized step data were integrated by the method of Lehmann and Larsen (1974) with background manually reset when necessary. Corrections were made for Lorentz and polarization effects, and for X-ray absorption by the crystal. In addition, corrections were made for absorption by the diamond and beryllium components of the pressure cell. Reflections having intensities greater than  $2\sigma(I)$  were considered as observed and were included in refinements, where  $\sigma(I)$  is the standard deviation determined from the counting statistics.

The initial structural model of wadsleyite was taken from Finger et al. (1993). Least-squares refinements were carried out using an updated version of RFIN4 (Finger and Prince 1975) in space group *Imma*. Neutral atomic scattering factors, including anomalous dispersion corrections for Fe, Si, and O, were taken from Ibers and Hamilton (1974). Anisotropic refinements were made for all data sets. Weighting schemes were based on  $w = [s^2(F) + (pF)^2]^{-1}$ , where  $p$  is adjusted to ensure that the errors were normally distributed through probability plot analysis (Ibers and Hamilton 1974). Type II isotropic extinction corrections (Becker and Coppens 1975) were applied in the refinements. Unit-cell dimensions and final refinement statistics are reported in Table 1. Atomic positional and isotropic displacement parameters are listed in Table 2, selected interatomic distances along with polyhedral volumes and

distortion indices are presented in Table 3, and selected interatomic angles appear in Table 4.

## RESULTS AND DISCUSSION

### Unit-cell parameters

Room-pressure unit-cell parameters of  $\beta\text{-(Fe}_{1.67}^{2+}\text{Fe}_{0.33}^{3+})(\text{Fe}_{0.33}^{3+}\text{Si}_{0.67})\text{O}_4$  are  $a = 5.8490(5)$ ,  $b = 11.8557(5)$ ,  $c = 8.3772(5)$  Å, and  $V = 580.91(7)$  Å<sup>3</sup>. These values differ significantly from those of a hypothetical  $\beta\text{-Fe}_2\text{SiO}_4$ , whose extrapolated unit-cell is  $a = 5.784$ ,  $b = 11.660$ ,  $c = 8.437$  Å, and  $V = 568.6$  Å<sup>3</sup>, based on values for a series of Mg-Fe wadsleyites reported by Finger et al. (1993). The substitution of  $2\text{Fe}^{3+}$  for  $\text{Fe}^{2+}$  + Si thus increases  $a$  and  $c$ , while decreasing  $b$ . This behavior is consistent with the fact that the  $b$ -axis dimension is constrained by chains of alternating, edge-sharing M1 and M2 octahedra, which become smaller with substitution of  $\text{Fe}^{3+}$  for  $\text{Fe}^{2+}$ . The  $a$  and  $c$  dimensions of the orthorhombic wadsleyite structure are more influenced by the size of the relatively rigid Si-bearing tetrahedral site, which becomes larger with  $\text{Fe}^{3+}$  substitution for Si.

These trends are supported by data of Woodland and Angel (1998), who report unit-cell parameters  $a = 5.8559$ ,  $b = 11.8936$ ,  $c = 8.3684$  Å, and  $V = 582.84$  Å<sup>3</sup> for  $\beta\text{-(Fe}_{1.55}^{2+}\text{Fe}_{0.45}^{3+})(\text{Fe}_{0.45}^{3+}\text{Si}_{0.55})\text{O}_4$ . Thus, the Woodland and Angel sample, which incorporates more ferric iron than our specimen, displays even larger  $a$  and  $c$  axes and a smaller  $b$  axis.

### Bulk moduli and linear compressibilities

Unit-cell volume and pressure data were fit to a third-order Birch-Murnaghan equation of state using program BMUR

**TABLE 1.** Crystal data and other relevant information for Fe<sup>3+</sup>-wadsleyite at various pressures

| <i>P</i> (GPa) | <i>a</i> (Å) | <i>b</i> (Å) | <i>c</i> (Å) | <i>V</i> (Å <sup>3</sup> ) | Refls. $>2\sigma(I)$ | <i>R</i> <sub>int</sub> <sup>*</sup> | <i>R</i> <sub>w</sub> <sup>†</sup> | <i>R</i> <sub>‡</sub> |
|----------------|--------------|--------------|--------------|----------------------------|----------------------|--------------------------------------|------------------------------------|-----------------------|
| 0.00           | 5.8490(5)    | 11.8557(5)   | 8.3772(5)    | 580.91(7)                  | 250                  | 0.022                                | 0.019                              | 0.025                 |
| 1.95           | 5.8286(5)    | 11.8205(5)   | 8.3481(4)    | 575.16(6)                  | 248                  | 0.023                                | 0.021                              | 0.024                 |
| 3.80           | 5.8076(4)    | 11.7804(5)   | 8.3147(4)    | 568.86(4)                  | 247                  | 0.022                                | 0.023                              | 0.026                 |
| 5.45           | 5.7889(3)    | 11.7496(3)   | 8.2898(4)    | 563.85(3)                  | 239                  | 0.023                                | 0.024                              | 0.025                 |
| 7.35           | 5.7721(4)    | 11.7214(4)   | 8.2658(4)    | 559.24(4)                  | 238                  | 0.024                                | 0.024                              | 0.026                 |
| 8.95           | 5.7557(5)    | 11.6949(4)   | 8.2433(5)    | 554.87(6)                  | 234                  | 0.026                                | 0.024                              | 0.025                 |

\* Residual for internal agreement of symmetry equivalent reflections.

†  $R_w = [\sum w(F_o - F_c)^2 / \sum wF_o^2]^{0.5}$ .

‡  $R = \sum |F_o - F_c| / \sum |F_o|$ .

**TABLE 2.** Atomic positional coordinates and isotropic displacement factors for Fe<sup>3+</sup>-wadsleyite at various pressures

| <i>P</i> (GPa) |          | 0.00      | 1.95      | 3.80      | 5.45      | 7.35      | 8.95      |
|----------------|----------|-----------|-----------|-----------|-----------|-----------|-----------|
| M1             | <i>B</i> | 0.67(5)   | 0.68(5)   | 0.69(4)   | 0.67(5)   | 0.67(5)   | 0.62(5)   |
|                | <i>z</i> | 0.9693(2) | 0.9699(2) | 0.9703(2) | 0.9706(2) | 0.9711(2) | 0.9715(2) |
| M2             | <i>B</i> | 0.51(4)   | 0.46(4)   | 0.51(4)   | 0.56(4)   | 0.59(4)   | 0.61(4)   |
|                | <i>z</i> | 0.1246(1) | 0.1245(1) | 0.1246(1) | 0.1245(1) | 0.1244(1) | 0.1244(1) |
| M3             | <i>B</i> | 0.71(3)   | 0.68(3)   | 0.68(3)   | 0.72(3)   | 0.75(3)   | 0.73(3)   |
|                | <i>z</i> | 0.1202(1) | 0.1202(1) | 0.1202(1) | 0.1204(1) | 0.1204(1) | 0.1204(1) |
| T              | <i>B</i> | 0.6179(2) | 0.6184(2) | 0.6183(2) | 0.6187(2) | 0.6191(2) | 0.6194(2) |
|                | <i>z</i> | 0.44(3)   | 0.45(3)   | 0.47(3)   | 0.47(3)   | 0.44(3)   | 0.42(3)   |
| O1             | <i>z</i> | 0.2257(8) | 0.2259(9) | 0.2272(9) | 0.2281(9) | 0.2282(9) | 0.2305(9) |
|                | <i>B</i> | 0.9(2)    | 0.9(2)    | 0.7(1)    | 0.7(2)    | 0.6(2)    | 0.7(2)    |
| O2             | <i>z</i> | 0.7207(8) | 0.7208(9) | 0.7237(9) | 0.7235(9) | 0.7251(9) | 0.7243(9) |
|                | <i>B</i> | 1.3(2)    | 1.6(2)    | 1.3(2)    | 1.2(2)    | 1.5(2)    | 1.3(2)    |
| O3             | <i>z</i> | 0.9920(3) | 0.9926(3) | 0.9931(3) | 0.9933(4) | 0.9935(4) | 0.9933(4) |
|                | <i>B</i> | 0.2548(7) | 0.2545(8) | 0.2548(8) | 0.2540(8) | 0.2535(9) | 0.2532(9) |
| O4             | <i>z</i> | 0.9(1)    | 1.1(1)    | 1.0(1)    | 1.2(1)    | 1.1(1)    | 1.2(1)    |
|                | <i>x</i> | 0.2579(4) | 0.2578(4) | 0.2578(4) | 0.2571(5) | 0.2579(5) | 0.2573(5) |
|                | <i>z</i> | 0.1223(2) | 0.1225(3) | 0.1227(3) | 0.1231(3) | 0.1234(3) | 0.1233(3) |
|                | <i>B</i> | 0.9991(4) | 0.9992(4) | 0.9996(4) | 0.9996(5) | 0.9989(5) | 0.9985(5) |
|                | <i>B</i> | 1.1(1)    | 1.0(1)    | 1.0(1)    | 0.9(1)    | 0.9(1)    | 1.0(1)    |

Notes: The following constraints apply to some atomic positional coordinates:  $x = y = z = 0$  for M1;  $x = 0$  and  $y = 1/4$  for M2, O1, and O2;  $x = z = 1/4$  for M3;  $x = 0$  for T and O3.

(Robert Downs, personal communication), which incorporates errors in both volume and pressure by employing the Levenberg-Marquardt least-squares method (Press et al. 1992). This procedure yields  $V_0 = 580.94(6) \text{ \AA}^3$ ,  $K_{70} = 173(3) \text{ GPa}$ , and  $K'_{70} = 5.2(9)$ . This bulk modulus is identical within experimental error to the 172(2) and 173(3) GPa values reported by Hazen et al. (2000) for  $\beta\text{-Mg}_2\text{SiO}_4$  and  $\beta\text{-(Mg}_{0.75}\text{Fe}_{0.25})_2\text{SiO}_4$ , respectively. The coupled substitution of  $2\text{Fe}^{3+}$  for Mg + Si thus appears to have no significant effect on bulk modulus.

Linear compressibilities, by contrast, do differ somewhat between  $\beta\text{-(Fe}_{1.67}^{2+}\text{Fe}_{0.33}^{3+})(\text{Fe}_{0.33}^{3+}\text{Si}_{0.67})\text{O}_4$  and  $\beta\text{-(Mg,Fe)}_2\text{SiO}_4$ . In Fe<sup>3+</sup>-wadsleyite, as in other wadsleyites, all unit-cell dimen-

sions (orthorhombic *a*, *b*, *c*, and *V*) decrease linearly with increasing pressure (Table 1; Fig. 1). Linear compressibilities of the *a*, *b*, and *c* axes ( $\beta_a$ ,  $\beta_b$ , and  $\beta_c$ ) are 0.00179(3), 0.00153(5), and 0.00180(5)/GPa, respectively, and the axial compression ratios ( $\beta_a$ :  $\beta_b$ :  $\beta_c$ ) are 1.17:1.00:1.18. In  $\beta\text{-(Mg,Fe)}_2\text{SiO}_4$ , for comparison,  $\beta_a$ ,  $\beta_b$ , and  $\beta_c$  are approximately 0.00145, 0.00145, and 0.00200/GPa, respectively (Hazen et al. 2000), which represents a significantly greater degree of compressional anisotropy ( $\beta_a$ :  $\beta_b$ :  $\beta_c \approx 1.0$ :1.0:1.4).

Note that in both normal and Fe<sup>3+</sup>-wadsleyite the *b* axis is least compressible, with  $\beta_b \approx 0.0015$ /GPa in both cases. The *c* axis, similarly, is the most compressible in both Fe<sup>3+</sup>- and nor-

**TABLE 3.** Selected interatomic distances (Å) and polyhedral distortion indices\* for Fe<sup>3+</sup>-wadsleyite at several pressures

| <i>P</i> (GPa) | 0.00      | 1.95      | 3.80      | 5.45      | 7.35      | 8.95      |
|----------------|-----------|-----------|-----------|-----------|-----------|-----------|
| M1-O3 ×2       | 2.137(6)  | 2.126(7)  | 2.120(7)  | 2.107(7)  | 2.097(7)  | 2.089(8)  |
| M1-O4 ×4       | 2.092(2)  | 2.087(3)  | 2.081(3)  | 2.075(3)  | 2.076(3)  | 2.067(3)  |
| M1 Average     | 2.107     | 2.100     | 2.094     | 2.086     | 2.083     | 2.074     |
| PV             | 12.45(3)  | 12.32(3)  | 12.23(3)  | 12.09(3)  | 12.03(4)  | 11.88(4)  |
| QE             | 1.0015(1) | 1.0013(1) | 1.0011(1) | 1.0009(1) | 1.0009(1) | 1.0010(1) |
| AV             | 4.7(1)    | 4.0(1)    | 3.4(1)    | 2.8(1)    | 3.1(1)    | 3.3(1)    |
| M2-O1          | 2.148(7)  | 2.137(8)  | 2.136(8)  | 2.135(9)  | 2.125(8)  | 2.135(9)  |
| M2-O2          | 2.083(7)  | 2.079(9)  | 2.050(9)  | 2.048(9)  | 2.033(9)  | 2.038(9)  |
| M2-O4 ×4       | 2.152(2)  | 2.142(3)  | 2.133(3)  | 2.120(3)  | 2.114(3)  | 2.107(3)  |
| M2 Average     | 2.140     | 2.131     | 2.120     | 2.111     | 2.103     | 2.100     |
| PV             | 12.88(3)  | 12.73(4)  | 12.53(4)  | 12.38(4)  | 12.25(4)  | 12.21(4)  |
| QE             | 1.0093(2) | 1.0090(2) | 1.0091(2) | 1.0089(2) | 1.0082(2) | 1.0077(2) |
| AV             | 32.5(3)   | 31.5(3)   | 31.5(3)   | 31.0(3)   | 28.5(3)   | 26.9(3)   |
| M3-O1 ×2       | 2.095(1)  | 2.089(1)  | 2.080(1)  | 2.074(1)  | 2.069(1)  | 2.063(1)  |
| M3-O3 ×2       | 2.147(3)  | 2.134(3)  | 2.124(3)  | 2.115(4)  | 2.106(4)  | 2.103(4)  |
| M3-O4 ×2       | 2.102(3)  | 2.094(3)  | 2.083(3)  | 2.076(4)  | 2.076(4)  | 2.074(4)  |
| M3 Average     | 2.115     | 2.106     | 2.095     | 2.088     | 2.084     | 2.080     |
| PV             | 12.55(2)  | 12.39(2)  | 12.21(2)  | 12.09(2)  | 12.02(2)  | 11.95(2)  |
| QE             | 1.0036(2) | 1.0034(2) | 1.0031(1) | 1.0028(2) | 1.0027(2) | 1.0023(2) |
| AV             | 12.4(2)   | 11.8(3)   | 10.7(3)   | 9.9(3)    | 9.4(3)    | 8.1(3)    |
| T-O2           | 1.763(4)  | 1.756(4)  | 1.762(4)  | 1.753(5)  | 1.754(5)  | 1.745(5)  |
| T-O3           | 1.705(5)  | 1.704(5)  | 1.701(5)  | 1.702(6)  | 1.700(6)  | 1.694(6)  |
| T-O4 (x2)      | 1.722(3)  | 1.720(3)  | 1.715(3)  | 1.715(4)  | 1.704(4)  | 1.702(4)  |
| T Average      | 1.728     | 1.725     | 1.723     | 1.721     | 1.716     | 1.711     |
| PV             | 2.64(1)   | 2.62(1)   | 2.62(1)   | 2.61(1)   | 2.58(1)   | 2.56(1)   |
| QE             | 1.0024(1) | 1.0025(2) | 1.0022(2) | 1.0023(2) | 1.0023(2) | 1.0024(2) |
| AV             | 10.0(3)   | 10.5(4)   | 9.0(4)    | 9.6(4)    | 9.4(4)    | 10.0(4)   |

\* PV = polyhedral volume; QE = quadratic elongation; AV = angle variance (Robinson et al. 1971).

**TABLE 4.** Selected interatomic angles for Fe<sup>3+</sup>-wadsleyite at several pressures

| <i>P</i> (GPa) | 0.00     | 1.95     | 3.80     | 5.45     | 7.35     | 8.95     |
|----------------|----------|----------|----------|----------|----------|----------|
| T-O2-T         | 121.5(4) | 121.8(5) | 120.4(5) | 120.6(5) | 120.1(5) | 120.6(5) |
| O2-T-O3        | 112.1(3) | 112.4(3) | 111.8(3) | 112.0(3) | 111.8(4) | 112.0(4) |
| O2-T-O4        | 105.4(1) | 105.3(2) | 105.6(2) | 105.5(2) | 105.6(2) | 105.4(2) |
| O3-T-O4        | 111.5(1) | 111.6(2) | 111.6(2) | 111.7(2) | 111.8(2) | 111.7(2) |
| O4-T-O4        | 110.6(2) | 110.3(2) | 110.2(2) | 110.2(3) | 110.1(3) | 110.3(3) |
| O3-M1-O4       | 92.0(1)  | 91.8(1)  | 91.6(1)  | 91.6(2)  | 91.7(1)  | 91.8(2)  |
| O3-M1-O4       | 88.0(1)  | 88.2(1)  | 88.4(1)  | 88.4(2)  | 88.3(1)  | 88.2(2)  |
| O4-M1-O4       | 87.7(1)  | 87.9(2)  | 88.0(2)  | 88.4(2)  | 88.3(2)  | 88.5(2)  |
| O4-M1-O4       | 92.3(1)  | 92.1(2)  | 92.0(2)  | 91.6(2)  | 91.7(2)  | 91.5(2)  |
| O1-M2-O4       | 83.3(1)  | 83.4(1)  | 83.4(1)  | 83.5(1)  | 83.8(1)  | 83.9(1)  |
| O2-M2-O4       | 96.7(1)  | 96.6(1)  | 96.6(1)  | 96.5(1)  | 96.2(1)  | 96.1(1)  |
| O4-M2-O4       | 89.4(1)  | 89.4(2)  | 89.3(2)  | 89.4(2)  | 89.1(2)  | 89.4(2)  |
| O4-M2-O4       | 89.0(1)  | 89.1(2)  | 89.2(2)  | 89.2(2)  | 89.5(2)  | 89.3(2)  |
| O1-M3-O1       | 89.6(1)  | 89.5(1)  | 89.5(1)  | 89.4(1)  | 89.3(1)  | 89.2(1)  |
| O1-M3-O3       | 92.6(1)  | 92.5(1)  | 92.4(1)  | 92.4(1)  | 92.4(1)  | 92.5(1)  |
| O1-M3-O4       | 85.8(2)  | 85.8(2)  | 86.1(2)  | 86.1(3)  | 86.1(3)  | 86.6(3)  |
| O1-M3-O4       | 95.2(2)  | 95.1(2)  | 94.8(2)  | 94.6(3)  | 94.3(3)  | 93.9(3)  |
| O3-M3-O3       | 85.9(1)  | 86.2(1)  | 86.3(1)  | 86.4(2)  | 86.5(2)  | 86.4(2)  |
| O3-M3-O4       | 91.4(2)  | 91.4(2)  | 91.5(2)  | 91.3(2)  | 91.4(2)  | 91.3(2)  |
| O3-M3-O4       | 87.5(2)  | 87.7(2)  | 87.6(2)  | 88.0(2)  | 88.1(2)  | 88.2(2)  |

mal wadsleyites, though the absolute compressibilities differ. The origins of these differences are revealed by variations of the crystal structure with pressure, which are described below.

### Cation ordering

The wadsleyite structure features three symmetrically independent octahedral sites (designated M1, M2, and M3) and one tetrahedral site (T). Half of Fe<sup>3+</sup> substitutes for Si on the T site; the mean T-O distance of 1.728 Å is reasonable for a site with average composition (Fe<sub>0.33</sub><sup>3+</sup>Si<sub>0.67</sub>). Similarly, Woodland and Angel (1998) report an average distance of 1.754 Å for their sample with T-site composition (Fe<sub>0.45</sub><sup>3+</sup>Si<sub>0.55</sub>). As in the previous study, we find that Fe<sup>3+</sup> and Si atoms are disordered on the tetrahedral site.

The remaining 0.33 Fe<sup>3+</sup> plus 1.67 Fe<sup>2+</sup> cations per formula unit are distributed over the three symmetrically distinct octahedral sites. Whereas X-ray analysis is not able to resolve Fe<sup>2+</sup>-Fe<sup>3+</sup> ordering directly, the extent of ferric-ferrous ordering can be estimated by comparing the observed M-O distances in the present study to those extrapolated from data for β-(Mg,Fe)<sub>2</sub>SiO<sub>4</sub> (Finger et al. 1993) to a hypothetical pure Fe<sup>2+</sup> end-member, β-Fe<sub>2</sub>SiO<sub>4</sub>. Average octahedral Fe<sup>3+</sup>-O distances are estimated by Shannon (1976) to be approximately 0.135 Å

shorter than average Fe<sup>2+</sup>-O bonds. The estimated Fe<sup>2+</sup>-O distances for M1, M2, and M3 extrapolated for β-Fe<sub>2</sub>SiO<sub>4</sub> are approximately 2.13, 2.12, and 2.14 Å, respectively. Here, we observe average Fe-O distances of 2.107, 2.140, and 2.115 Å; similarly, Woodland and Angel (1998) report 2.101, 2.134, and 2.100 Å.

The observed Fe-O distances for M2 are slightly larger than those predicted for a pure Fe<sup>2+</sup> end-member. We conclude, therefore, that M2 incorporates little, if any, ferric iron. Observed Fe-O distances for M1 and M3, by contrast, are approximately 0.025 Å shorter than predicted for a pure Fe<sup>2+</sup> phase. This shortening could be explained by 22% occupancy of Fe<sup>3+</sup> in both M1 and M3. That degree of occupancy would explain the shorter than predicted Fe-O distances, while achieving the required (Fe<sub>1.67</sub><sup>2+</sup>Fe<sub>0.33</sub><sup>3+</sup>) average octahedral composition (note that the multiplicities of M1 and M2 are 4, while those of M3 and T are 8). Mössbauer spectroscopic analysis of these samples could further resolve this assumed cation ordering.

The reason for Fe<sup>3+</sup> avoidance of the M2 site may relate to the relative sizes and distortions of the three distinct cation octahedra. Ferrous iron normally occupies the largest and most distorted octahedral site, which is the M2 octahedron in β-(Fe<sub>1.67</sub><sup>2+</sup>Fe<sub>0.33</sub><sup>3+</sup>)(Fe<sub>0.33</sub><sup>3+</sup>Si<sub>0.67</sub>)O<sub>4</sub>. Note, however, that in β-

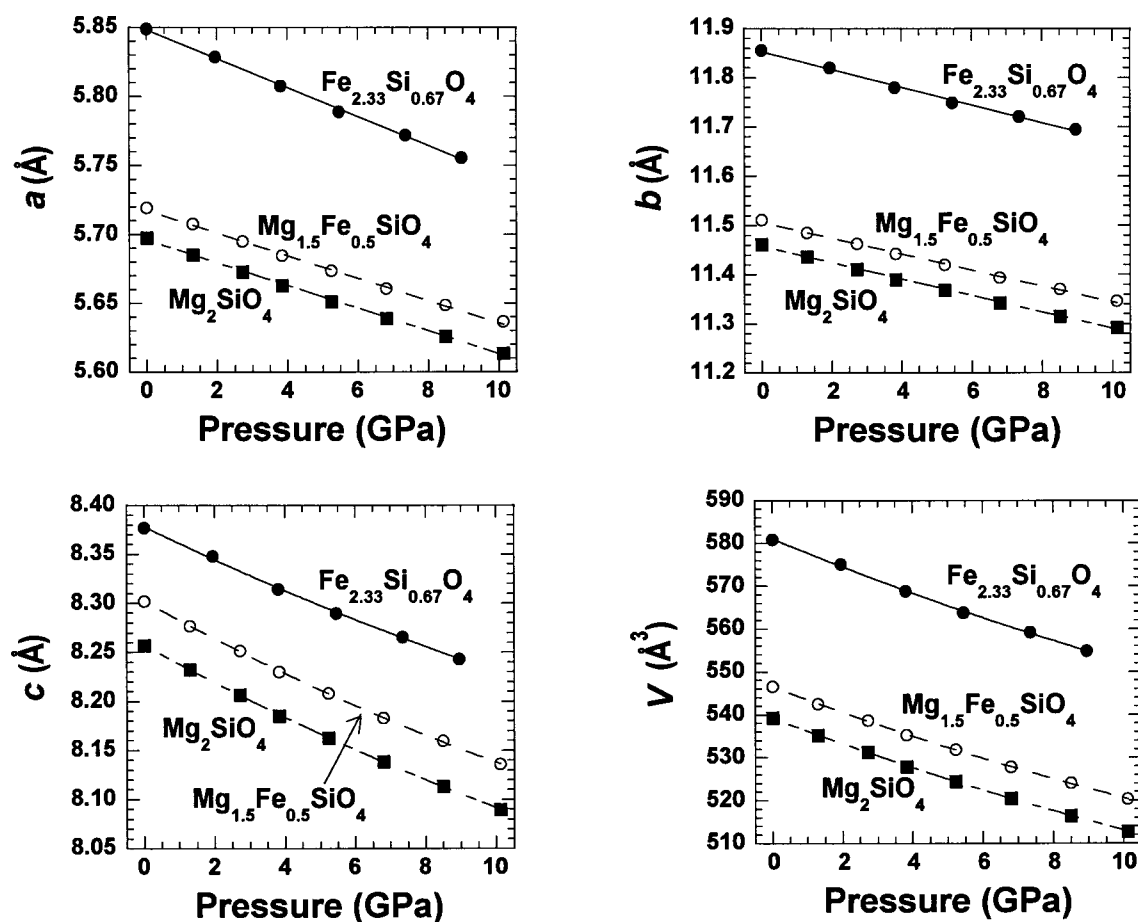


FIGURE 1. The variation of orthorhombic unit-cell parameters for three wadsleyites with pressure. Samples include Fe<sub>2.33</sub>Si<sub>0.67</sub>O<sub>4</sub> from this study, and Mg<sub>2</sub>SiO<sub>4</sub> and Mg<sub>1.5</sub>Fe<sub>0.5</sub>SiO<sub>4</sub> from Hazen et al. (2000).

(Mg,Fe)<sub>2</sub>SiO<sub>4</sub> Fe<sup>2+</sup> strongly favors M1 and M3 compared to M2, which is intermediate in size and distortion in that phase. The Fe<sup>3+</sup> octahedral site preference in an Mg-rich wadsleyite is, therefore, not obvious.

Ferric-ferrous ordering in Fe<sup>3+</sup>-wadsleyite may also be influenced by local electrostatic balance. M2 is the only octahedron that is coordinated to O2, which is the bridging oxygen of the Si<sub>2</sub>O<sub>7</sub> dimer in wadsleyite. O2 is already significantly overbonded (Smyth 1994) and substitution of Fe<sup>3+</sup> for a divalent M2 cation would tend to exacerbate this O2 overbonding. By the same token, the O1 oxygen, which shares four M3 and one M1 octahedra, and the O3 oxygen, which shares M1, M3, and T polyhedra, are significantly underbonded (Smyth 1994). Substitution of Fe<sup>3+</sup> into M1 or M3, therefore, would help to alleviate both O1 and O3 underbonding.

### Structural variations with pressure—the T site

Examination of crystal structures determined at six pressures to 8.95 GPa reveals systematic variations in cation-oxygen distances. These data lend support to the cation ordering scheme proposed above. In particular, substitution of trivalent cations into octahedral and tetrahedral sites of β-(Fe<sub>1.67</sub><sup>2+</sup>Fe<sub>0.33</sub><sup>3+</sup>)(Fe<sub>0.33</sub><sup>3+</sup>Si<sub>0.67</sub>)O<sub>4</sub> systematically alters the sizes and bulk moduli of those cation polyhedra.

In Fe<sup>3+</sup>-wadsleyite the observed bulk modulus of the T site with average composition (Fe<sub>0.33</sub><sup>3+</sup>Si<sub>0.67</sub>) is 315(47) GPa. This value is less than the 350 GPa bulk modulus observed for the pure-Si T site in β-(Mg,Fe)<sub>2</sub>SiO<sub>4</sub> (Hazen et al. 2000). Thus, as predicted from crystal chemical systematics (Hazen and Finger 1982), the T site of Fe<sup>3+</sup>-wadsleyite is larger and more compressible than the T site of its Fe<sup>2+</sup> counterpart.

Tetrahedral distortion indices (Table 3) and O-T-O angles do not change significantly with pressure. Individual tetrahedra thus behave as relatively rigid structural units. Pairs of tetrahedra in wadsleyite form a dimer that is linked by a bridging O2 oxygen. The T-O2-T angle thus provides a useful measure of lattice distortion during compression (Table 4). In the present study, as in the previous high-pressure investigation of β-(Mg,Fe)<sub>2</sub>SiO<sub>4</sub> (Hazen et al. 2000), this angle is observed to undergo a small but significant decrease of approximately 1° between room pressure and 9 GPa. This T-O2-T bending contributes slightly to wadsleyite compression parallel to the *b* axis.

### Structural variations with pressure—the M sites

All Fe-O bonds display significant shortening with pressure (Table 3, Fig. 2). The M2 site, which is the largest octahedral site and presumably the one with the least ferric iron (see above), displays the smallest polyhedral bulk modulus, 163(12) GPa. This value is identical to the average bulk moduli of divalent cation octahedra in β-(Mg<sub>0.75</sub>Fe<sub>0.25</sub>)<sub>2</sub>SiO<sub>4</sub> (Hazen et al. 2000)—an observation that lends support to the Fe<sup>2+</sup>-Fe<sup>3+</sup> ordering scheme proposed above.

Both M1 and M3 have significantly greater octahedral bulk moduli than M2: 202(10) and 185(17) GPa, respectively. These values are greater than bulk moduli of divalent cation octahedra observed in β-(Mg,Fe)<sub>2</sub>SiO<sub>4</sub>, but are similar to the 190 GPa bulk modulus of the mixed Fe<sup>2+</sup>-Fe<sup>3+</sup> octahedron in magnetite (Finger et al. 1986). We suggest that the greater octahedral bulk

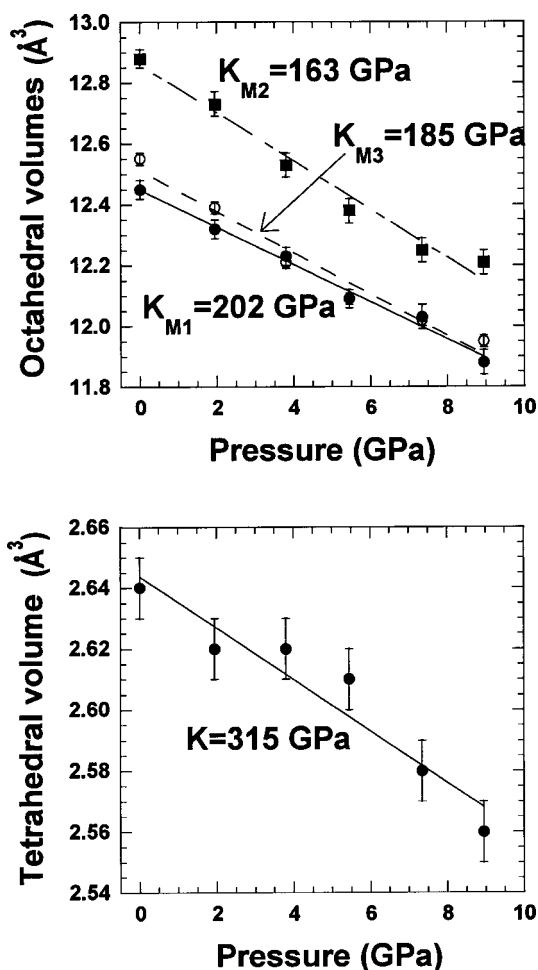


FIGURE 2. Polyhedral volumes versus pressure for three cation octahedra and one tetrahedron in Fe<sup>3+</sup>-wadsleyite.

moduli of M1 and M3 reflect the presence of significant Fe<sup>3+</sup> in these two sites. Ferric iron tends to decrease both the size and the compressibility of iron-bearing octahedral sites compared to ferrous iron (e.g., Hazen and Finger 1982).

In Fe<sup>3+</sup>-wadsleyite, as in β-(Mg,Fe)<sub>2</sub>SiO<sub>4</sub>, all three cation octahedra become significantly more regular with increasing pressure. Both quadratic elongation and angle variances of M1, M2, and M3 decrease, which suggests that the close-packed oxygen array becomes more regular under compression.

### Compression mechanisms

The anisotropy of unit-cell compression in β-(Fe<sub>1.67</sub><sup>2+</sup>Fe<sub>0.33</sub><sup>3+</sup>)(Fe<sub>0.33</sub><sup>3+</sup>Si<sub>0.67</sub>)O<sub>4</sub> reflects anisotropy in the compression of individual Fe-O bonds, as well as the relative compressibilities of its four cation polyhedra. The *b* axis is the least compressible, as in other wadsleyites, because it is parallel to the relatively rigid tetrahedral dimers. The *c* axis is the most compressible, as in other wadsleyites, because that direction is parallel to the most compressible octahedral Fe-O bonds: M1-O3 and M2-O2.

Despite these similarities, the presence of ferric iron in both tetrahedral and octahedral sites reduces the compressional anisotropy of Fe<sup>3+</sup>-wadsleyite compared to β-(Mg,Fe)<sub>2</sub>SiO<sub>4</sub>. In

$\beta$ -Mg<sub>2</sub>SiO<sub>4</sub> the tetrahedral bulk modulus is 350 GPa, while that of the average octahedral site (with appropriate weighting for site multiplicities) is 145 GPa. In  $\beta$ -(Fe<sub>1.67</sub><sup>2+</sup>Fe<sub>0.33</sub><sup>3+</sup>)(Fe<sub>0.33</sub><sup>3+</sup>Si<sub>0.67</sub>)O<sub>4</sub>, by contrast, T and M bulk moduli are 315 and 184 GPa, respectively. Ferric iron reduces the bulk modulus of the pure Si T site, and it increases the bulk moduli of the nominally divalent M sites. The contrast between tetrahedral and octahedral bulk moduli is diminished, and thus all modules of the structure compress more uniformly.

### CONCLUSIONS

The high-pressure crystal chemistry of Fe<sup>3+</sup>-wadsleyite underscores the importance of documenting the range of possible compositional variations, as well as the effect of those variations on physical properties, in presumed mantle phases. In the case of  $\beta$ -(Fe<sub>1.67</sub><sup>2+</sup>Fe<sub>0.33</sub><sup>3+</sup>)(Fe<sub>0.33</sub><sup>3+</sup>Si<sub>0.67</sub>)O<sub>4</sub>, the substitution of ferric iron has little effect on bulk modulus, but the presence of Fe<sup>3+</sup> significantly alters axial compressibilities and, presumably, shear moduli, as well.

In wadsleyite, the uncertainties in physical properties associated with compositional variations are compounded by Mg-Fe<sup>2+</sup>-Fe<sup>3+</sup> cation ordering. Mg-Fe ordering (Hazen et al. 2000) and Fe<sup>2+</sup>-Fe<sup>3+</sup> ordering (this study) have significant effects on the relative compressibilities of the three symmetrically independent cation octahedra, and thus on the compressional anisotropy of wadsleyite. As cation ordering patterns change with temperature, pressure, and composition, so, too, will wadsleyite's physical properties. Under such circumstances, in situ characterization of equilibrated samples at appropriate temperature and pressure may provide the only valid procedure to obtain relevant structural and physical properties of mantle phases.

### ACKNOWLEDGMENTS

We thank Y. Fei for providing the wadsleyite sample, which was synthesized at the high-pressure multi-anvil laboratory of the Geophysical Laboratory, which is jointly sponsored by the NSF Center for High Pressure Research and the Carnegie Institution of Washington. Crystallographic studies are supported by NSF grant EAR-9805282, the Center for High Pressure Research, and by the Carnegie Institution of Washington.

### REFERENCES CITED

- Anderson, D.L. (1970) Petrology of the mantle. Mineralogical Society of America Special paper, 3, 85–93.
- Becker, P.J. and Coppens, P. (1975) Extinction within the limit of validity of the Darwin transfer equations: III. Non-spherical crystals and anisotropy of extinction. *Acta Crystallographica*, A31, 417–425.
- Bell, D.R. and Rossman, G.R. (1992) Water in Earth's mantle: The role of nominally anhydrous minerals. *Science*, 255, 1391–1396.
- Bina, C.R. and Wood, B.J. (1987) Olivine-spinel transitions: experimental and thermodynamic constraints and implications for the nature of the 400 km seismic discontinuity. *Journal of Geophysical Research*, 92, 4853–4866.
- Downs, J.W. (1989) Possible sites for protonation in  $\beta$ -Mg<sub>2</sub>SiO<sub>4</sub> from an experimentally derived electrostatic potential. *American Mineralogist*, 74, 1124–1129.
- Fei, Y. and Bertka, C.M. (1996) The  $\alpha$ - $\beta$  transition in systems relevant to the upper mantle. *EOS Transactions of the American Geophysical Union*, 77, 649.
- Finger, L.W. and King, H. (1978) A revised method of operation of the single-crystal diamond cell and refinement of the structure of NaCl at 32 kbar. *American Mineralogist*, 63, 337–342.
- Finger, L.W. and Prince, E. (1975) A system of FORTRAN IV computer programs for crystal structure computations. National Bureau of Standards Technology Note 854.
- Finger, L.W., Hazen, R.M., and Hofmeister, A.M. (1986) High-pressure crystal chemistry of spinel (MgAl<sub>2</sub>O<sub>4</sub>) and magnetite (Fe<sub>3</sub>O<sub>4</sub>): comparisons with silicate spinels. *Physics and Chemistry of Minerals*, 13, 215–220.
- Finger, L.W., Hazen, R.M., Zhang, J., Ko, J., and Navrotsky, A. (1993) The effect of Fe on the crystal structure of wadsleyite,  $\beta$ -(Mg<sub>1-x</sub>Fe<sub>x</sub>)<sub>2</sub>SiO<sub>4</sub>, 0.00 < x < 0.40. *Physics and Chemistry of Minerals*, 19, 361–368.
- Haiber, M., Ballone, P., and Parrinello, M. (1997) Structure and dynamics of protonated Mg<sub>2</sub>SiO<sub>4</sub>: An ab-initio molecular dynamics study. *American Mineralogist*, 82, 913–922.
- Hazen, R.M. and Finger, L.W. (1982) *Comparative Crystal Chemistry*. Wiley, New York.
- Hazen, R.M., Weinberger, M.B., Yang, H., and Prewitt, C.T. (2000) Comparative high-pressure crystal chemistry of wadsleyite,  $\beta$ -(Mg<sub>1-x</sub>Fe<sub>x</sub>)<sub>2</sub>SiO<sub>4</sub>, with x = 0 and 0.25. *American Mineralogist*, 85, 775–782.
- Helffrich, G.R. and Wood, B.J. (1996) 410 km discontinuity sharpness and the form of the olivine  $\alpha$ - $\beta$  phase diagram: resolution of apparent seismic contradictions. *Geophysical Journal International*, 126, F7–F12.
- Ibers, J.A. and Hamilton, W.C. (1974) *International tables for X-ray crystallography*. Vol. IV, 366 p. Kynoch, Birmingham, U.K.
- Inoue, T. (1994) Effect of water on melting phase-relations and melt composition in the system Mg<sub>2</sub>SiO<sub>4</sub>-MgSiO<sub>3</sub>-H<sub>2</sub>O up to 15 GPa. *Physics of the Earth and Planetary Interiors*, 85, 237–245.
- Irfune, T. and Isshiki, M. (1998) Iron partitioning in a pyrolite mantle and the nature of the 410-km seismic discontinuity. *Nature*, 392, 702–704.
- Ita, J. and Stixrude, L. (1992) Petrology, elasticity, and composition of the mantle transition zone. *Journal of Geophysical Research*, 97, 6849–6866.
- Jeanloz, R. and Thompson, A.B. (1983) Phase transition and mantle discontinuities. *Reviews in Geophysics and Space Physics*, 21, 51–74.
- King, H.E. and Finger, L.W. (1979) Diffracted beam crystal centering and its application to high pressure crystallography. *Journal of Applied Crystallography*, 12, 374–378.
- Kudoh, Y. and Inoue, T. (1999) Mg-vacant structural modules and dilution of the symmetry of hydrous wadsleyite,  $\beta$ -Mg<sub>2-x</sub>SiH<sub>2x</sub>O<sub>4</sub> with 0.00 < x < 0.25. *Physics and Chemistry of Minerals*, 26, 382–388.
- Kudoh, Y., Inoue, T., and Arashi, H. (1996) Structure and crystal chemistry of hydrous wadsleyite Mg<sub>1.75</sub>SiH<sub>0.5</sub>O<sub>4</sub>: Possible hydrous magnesium silicate in the mantle transition zone. *Physics and Chemistry of Minerals*, 23, 461–469.
- Lehmann, M.S. and Larsen, F.K. (1974) A method for location of the peaks in step-scan-measured Bragg reflexions. *Acta Crystallographica*, A30, 580–584.
- Mao, H.K., Xu, J., and Bell, P.M. (1986) Calibration of the ruby pressure gauge to 800 kbar under quasi-hydrostatic conditions. *Journal of Geophysical Research*, 91, 4673–4676.
- Ohtaka, O., Tobe, H., and Yamanaka, T. (1997) Phase equilibria for the Fe<sub>2</sub>SiO<sub>4</sub>-Fe<sub>3</sub>O<sub>4</sub> system under high pressure. *Physics and Chemistry of Minerals*, 24, 555–560.
- O'Neill, H.St.C., Rubie, D.C., Canil, D., Geiger, C.A., Ross, C.R., II, Seifert, F., and Woodland, A. (1993) Ferric iron in the upper mantle and in transition zone assemblages: Implications for relative oxygen fugacities in the mantle. *Evolution of the Earth and Planets (Geophysical Monograph 74, IUGG Volume 14)*, 73–88.
- Press, W.H., Teukolsky, S.K., Vetterling, W.T., and Flannery, B.P. (1992) *Numerical Recipes in Fortran 77*. Cambridge, Cambridge University Press, U.K.
- Robinson, K., Gibbs, G.V., and Ribbe, P.H. (1971) Quadratic elongation: A quantitative measure of distortion in coordination polyhedra. *Science*, 172, 567–570.
- Ross, C.R. II, Armbruster, T., and Canil, D. (1992) Crystal structure of a spinelloid in the system Fe<sub>2</sub>O<sub>3</sub>-Fe<sub>2</sub>SiO<sub>4</sub>. *American Mineralogist*, 77, 507–511.
- Shannon, R. (1976) Revised effective ionic radii and systematic studies of interatomic distances in halides and chalcogenides. *Acta Crystallographica*, A32, 751–767.
- Slesinger, A., Bertka, C.M., and Fei, Y. (1997) Phase relations in the Fe<sub>2</sub>SiO<sub>4</sub>-Fe<sub>3</sub>O<sub>4</sub> system at high pressures. *EOS Transactions of the American Geophysical Union*, 78, F766.
- Smyth, J.R. (1987)  $\beta$ -Mg<sub>2</sub>SiO<sub>4</sub>: a potential host for water in the mantle? *American Mineralogist*, 72, 1051–1055.
- (1994) A crystallographic model for hydrous wadsleyite ( $\beta$ -Mg<sub>2</sub>SiO<sub>4</sub>): an ocean in the Earth's interior? *American Mineralogist*, 79, 1021–1024.
- Smyth, J.R. and Kawamoto, T. (1997) Wadsleyite II: A new high pressure hydrous phase in the peridotite-H<sub>2</sub>O system. *Earth and Planetary Science Letters*, 146, E9–E16.
- Smyth, J.R., Kawamoto, T., Jacobsen, S.D., Swope, R.J., Hervig, R.L., and Holloway, J.R. (1997) Crystal Structure of monoclinic hydrous wadsleyite [ $\beta$ -(Mg,Fe)<sub>2</sub>SiO<sub>4</sub>]. *American Mineralogist*, 82, 270–275.
- Woodland, A.B. and Angel, R.J. (1998) Crystal structure of a new spinelloid with the wadsleyite structure in the system Fe<sub>2</sub>SiO<sub>4</sub>-Fe<sub>3</sub>O<sub>4</sub> and implications for the Earth's mantle. *American Mineralogist*, 83, 404–408.
- Young, T.E., Green, H.W., Hofmeister, A.M., and Walker, D. (1993) Infrared spectroscopic investigation of hydroxyl in  $\beta$ -(Mg,Fe)<sub>2</sub>SiO<sub>4</sub> and coexisting olivine: implications for mantle evolution and dynamics. *Physics and Chemistry of Minerals*, 19, 409–422.

MANUSCRIPT RECEIVED JULY 26, 1999

MANUSCRIPT ACCEPTED DECEMBER 20, 1999

PAPER HANDLED BY JAMES W. DOWNS